EUROPEAN SYNCHROTRON RADIATION FACILITY

INSTALLATION EUROPEENNE DE RAYONNEMENT SYNCHROTRON

ESRF

Experiment Report Form

The double page inside this form is to be filled in by all users or groups of users who have had access to beam time for measurements at the ESRF.

Once completed, the report should be submitted electronically to the User Office using the **Electronic Report Submission Application:**

http://193.49.43.2:8080/smis/servlet/UserUtils?start

Reports supporting requests for additional beam time

Reports can now be submitted independently of new proposals – it is necessary simply to indicate the number of the report(s) supporting a new proposal on the proposal form.

The Review Committees reserve the right to reject new proposals from groups who have not reported on the use of beam time allocated previously.

Reports on experiments relating to long term projects

Proposers awarded beam time for a long term project are required to submit an interim report at the end of each year, irrespective of the number of shifts of beam time they have used.

Published papers

All users must give proper credit to ESRF staff members and proper mention to ESRF facilities which were essential for the results described in any ensuing publication. Further, they are obliged to send to the Joint ESRF/ ILL library the complete reference and the abstract of all papers appearing in print, and resulting from the use of the ESRF.

Should you wish to make more general comments on the experiment, please note them on the User Evaluation Form, and send both the Report and the Evaluation Form to the User Office.

Deadlines for submission of Experimental Reports

- 1st March for experiments carried out up until June of the previous year;
- 1st September for experiments carried out up until January of the same year.

Instructions for preparing your Report

- fill in a separate form for each project or series of measurements.
- type your report, in English.
- include the reference number of the proposal to which the report refers.
- make sure that the text, tables and figures fit into the space available.
- if your work is published or is in press, you may prefer to paste in the abstract, and add full reference details. If the abstract is in a language other than English, please include an English translation.

ESRF	**Experiment title:** Dynamics of Capillarity and Fluidisation in Wet Granular Media	**Experiment number**: ME-1044
Beamline: ID 15A	**Date of experiment**: from: 18.05.2005 to: 22.05.2005	**Date of report**:
Shifts: 18	**Local contact(s)**: Marco DiMichiel	*Received at ESRF:* *15*

Names and affiliations of applicants (* indicates experimentalists):

Ralf Seemann*, MPI for Dynamics and Self-Organization, Goettingen, Germany

Mario Scheel*, MPI for Dynamics and Self-Organization, Goettingen, Germany,

Stephan Herminghaus*, MPI for Dynamics and Self-Organization, Goettingen, Germany

Klaus Mecke, University of Erlangen, Erlangen, Germany

Report:

The mechanical properties of granulates change dramatically if some liquid is added. Typically a stiffening of the granulate is observed. The main reason is the internal cohesion due to capillary forces arising from liquid bridges between the grains [1-11]. The aim of our current experiments was to get an insight into the three dimensional distribution of the liquid. On the long run we hope to correlate the liquid distribution with the mechanical properties of the granulate. Hence, we imaged wet granulates in 3D whereas the clear distinction of the air, the liquid and the granules by the x-ray absorption contrast was crucial. For simplicity, we used model granulates consisting of glass spheres with diameter ranging from about 180 to 550 µm, that show the same qualitative behavior than "real" granulates like sand. As a wetting liquid we used a mixture of water and NaI to increase the x-ray absorption. Using the fast x-ray tomography setup at ID 15A imaging of wet granulates was possible with sufficient lateral resolution and a clear distinction of the air, the liquid and the glass, which allows for a detailed and quantitative analysis of the data. Even slow dynamic processes could be recorded by capturing fast series of x-ray tomograms or 2D projections, as we will demonstrate in the following on the basis of preliminary data analysis.

In a first set of experiments we measured the static distribution of liquid bridges and clusters as a function of liquid content, packing density, and sphere size. Figure 1a shows an example of densely packed glass spheres of about 275 µm diameter for various liquid contents. The number of liquid bridges per sphere as a function of liquid content obtained from x-ray tomograms nicely continue the data obtained by an optical index matching technique towards larger liquid contents [9, 11], as shown in fig. 1b. If a small amount of liquid is added to a granulate liquid bridges are formed leading to a remarkable stiffening of the granulate. For increasing liquid content the bridges per sphere stay about constant for more than one order of magnitude. When the liquid content exceeds 1 %, the number of liquid bridges is reduced and the liquid forms liquid clusters that finally span the full granulate (percolation threshold). Hence, for liquid contents larger than 1 % counting bridges is not sufficient any more and a more powerful tool is required to analyze the liquid

distribution within a granulate. We do this by means of Minkowski Measures [12, 13] as a function of liquid content [14]. To characterize the liquid distribution within the granulate in three dimensions we have to extract four measures out of the tomograms. The liquid volume, the surface area and the curvature of the liquid interface and the Euler characteristic, which is a measure of the connectivity of the liquid morphologies, cf. fig. 1c-e. The liquid volume is not shown in fig. 1 because it is well known from the sample preparation and was used to find the right parameters for the data analysis. Analogous, the same routine is used to analyze the packing geometry of the glass spheres by simply replacing liquid by glass. In a second step we would like to link the morphological data of wet granulates to their mechanical properties.

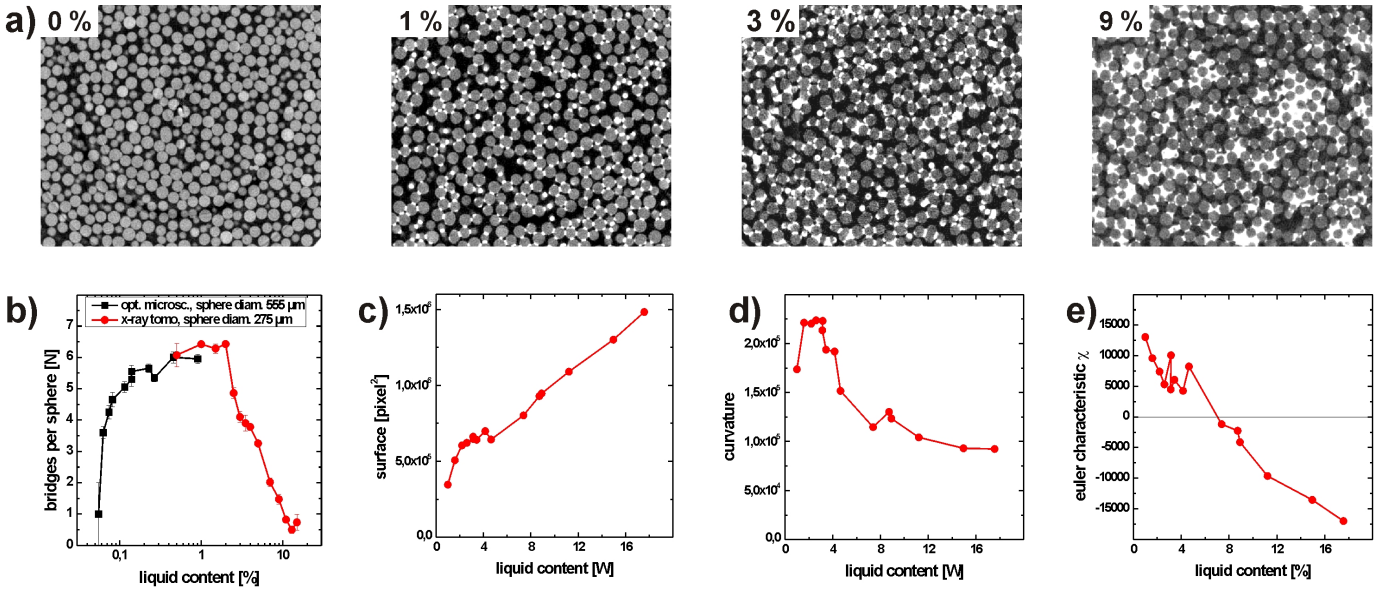

Figure 1: a) 2D slices of densely packed granulates. The liquid content in volume percent is given in the left upper corner. b) bridges per sphere as a function of liquid content. Data for low liquid content were obtained by an optical index matching technique (black squares), whereas data for larger liquid contents were obtained by x-ray tomography (red dots) c - e) Minkowski Measures as function of liquid content as obtained from x-ray tomograms [14]. c) area of the liquid interface, d) curvature of the liquid interface, e) Euler characteristic of the liquid distribution.

When a granulate is fluidized, e.g. by vertical agitation, liquid bridges and clusters break and the liquid is distributed along the surface of the spheres. When the agitation is stopped, the liquid morphologies will equilibrate while the stiffness of the wet granulate increases until an equlibrium distribution is restored. We used the good time resolution of the fast x-ray tomography setup to measure how the liquid bridges and clusters are restored after heavily fluidization the granulate. To reduce the delay between stopping the agitation and capturing the first tomogram, we mounted the sample on a loudspeaker, which was used to fluidize the granulate and which was mounted on the rotational stage of the tomography setup. In figure 2a the change in volume of individual bridges is shown after stopping the vertical agitation. Large bridges shrink in size whereas small bridges grow, resulting in fairly well defined mean bridge volume that is given by the liquid content, the sphere size, and the packing geometry. The exponential growth or shrinkage rates fit perfectly to values obtained by optical techniques for smaller liquid contents and larger viscosities [9].

To visualize the movement of individual spheres within a fluidized granulate we mounted the sample on a loudspeaker as described before but continued the agitation when capturing images. Using tracer particles with large x-ray absorption comntrast, like gold or BaTi spheres, we can clearly identify their positions on a 2D projection, see fig. 3a. If we capture two 2D projections from different observation angles, without significant change in the position of the sphere within the sample, we can easily derive the 3D position of a tracer sphere, as depicted in the sketch of fig. 3b. Repeating this process continuously we can record 3D flight passes of tracer particles within a fluidized granulate. Moving speeds of up to 250 µm/s can be recorded easily with good lateral resolution, provided the amplitude of the agitation is not too large.

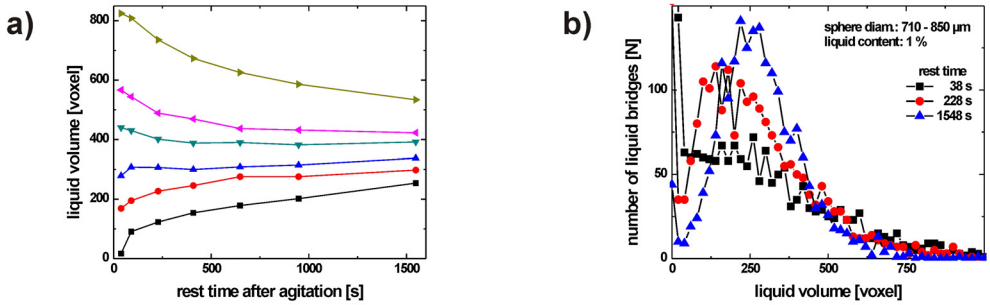

Figure 2: Equilibration of liquid bridges after fluidizing the granulate [15]. Sphere size: 710 - 850 µm, liquid content 1 % a) volume change of individual liquid bridges. b) sum of liquid bridge volumes as function of bridge volume taken at three different resting times. The liquid bridge distribution narrows and shifts to larger values after some resting time.

Analogous, large size differences of individual spheres can be used to trace them e.g. in case of the Brazil nut effect [16]. The Brazil nut effect could be visualized for wet and dry granulates where a different fluidization behavior of wet granulates compared to dry granulates could be found. For a dry granulate on a larger scale we typically found that the spheres follow the collective movement of a convection roll. For wet granulates a convection roll could be found for very large agitation amplitudes, only. In case of wet granulates, we rather found indications for a Leidenfrost-phenomena, where a "liquid" plug coexists with a "gaseous" layer between the bottom of the sample vial and the liquid plug. To decide whether there is an additional diffusive movement or catching of the individual spheres on a smaller length scale, a more detailed analysis of the data is reqired. As preliminary result a short flight pass is shown in fig. 3c. The periodic fluctuations are due to an incomplete correction of the rotational movement of the sample cell.

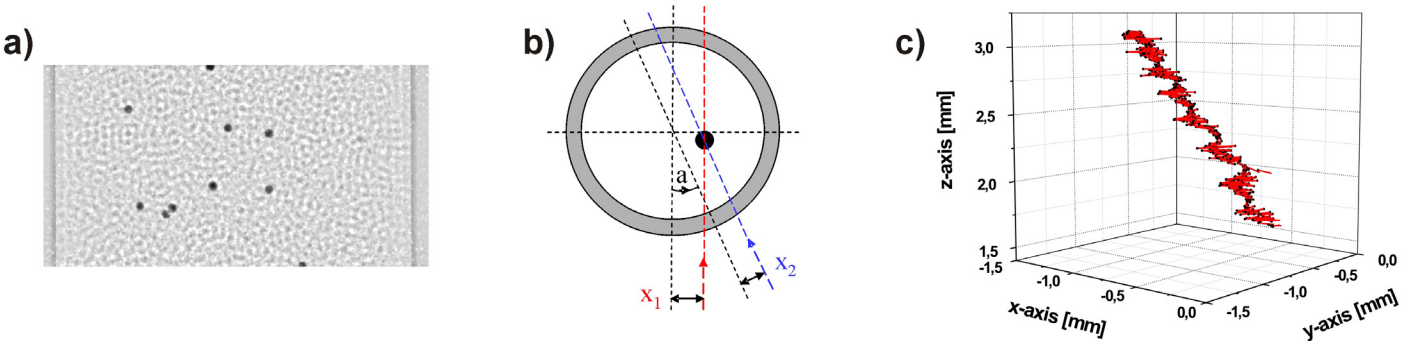

Figure 3: a) typical 2D projection in binning mode using BaTi tracer spheres b) sketch how to obtain a 3D position of a tracer sphere from two 2D projections, taken at different view points c) preliminary reconstructed flight pass of a tracer sphere with an average speed of 89 µm/s.

[1] D. J. Hornbaker, R. Albert, I. Albert, A.-L. Barabasi, and P. Schiffer, *Nature* **387**, 765 (1997)
[2] T. C. Halsey and A. J. Levine, *Phys. Rev. Lett.* **80**, 3141 (1998)
[3] L. Bocquet, E. Charlaix, S. Ciliberto, and J. Crassous, *Nature* **396**, 735 (1998)
[4] N. Fraysee, H. Thomé, and L. Petit, *Eur. Phys. J. B* **11**, 615 (1999)
[5] R. R. Hartley and R. P. Behringer, *Nature* **421**, 928 (2003)
[6] G. Ovalez, E. Kolb, and E. Clement, *Phys. Rev. E* **64**, 060302(R) (2001)
[7] D. Geromichalos, M. M. Kohonen, F. Mugele, and S. Herminhaus, *Phys. Rev. Lett.* **90**, 168702 (2003)
[8] S. Herminghaus, *Advances in Physics* **54**, 221 (2005)
[9] M. M. Kohonen, D. Geromichalos, M. Scheel, C. Schier, and S. Herminghaus, *Physica A* **339** (2004) 7
[10] M. Scheel, D. Geromichalos, and S. Herminghaus, J. Phys.: Condens. Matter **16**, S4213 (2004)
[11] Z. Fournier, et al., *J. Phys.: Condens. Matter* **17** (2005) S477
[12] K. R. Mecke, *Int. J. Mod. Phys. B* **12**, 861 (1998)
[13] K. R. Mecke and D. Stoyan, Lecture Notes in Physics Vol. 554 (Springer, Berlin, 2000)
[14] M. Scheel, B. Breitenbach, K. R. Mecke, M. DiMichiel, S. Herminghaus, R. Seemann, *to be published*
[15] M. Scheel, M. DiMichiel, S. Herminghaus, R. Seemann, *to be published*
[16] G. H. Ristow, *Pattern Formation in Granular Materials* (Springer, Berlin, 2000)